

**Health Assessment and Fault Classification of Roller
Element Bearings**

by Andrew J. Bayba, David N. Siegel, Kwok Tom, and Derwin Washington

ARL-TR-6080

July 2012

NOTICES

Disclaimers

The findings in this report are not to be construed as an official Department of the Army position unless so designated by other authorized documents.

Citation of manufacturer's or trade names does not constitute an official endorsement or approval of the use thereof.

Destroy this report when it is no longer needed. Do not return it to the originator.

Army Research Laboratory

Adelphi, MD 20783-1197

ARL-TR-6080

July 2012

Health Assessment and Fault Classification of Roller Element Bearings

Andrew J. Bayba, David N. Siegel, Kwok Tom, and Derwin Washington
Sensors and Electron Devices Directorate, ARL

REPORT DOCUMENTATION PAGE

Form Approved
OMB No. 0704-0188

Public reporting burden for this collection of information is estimated to average 1 hour per response, including the time for reviewing instructions, searching existing data sources, gathering and maintaining the data needed, and completing and reviewing the collection information. Send comments regarding this burden estimate or any other aspect of this collection of information, including suggestions for reducing the burden, to Department of Defense, Washington Headquarters Services, Directorate for Information Operations and Reports (0704-0188), 1215 Jefferson Davis Highway, Suite 1204, Arlington, VA 22202-4302. Respondents should be aware that notwithstanding any other provision of law, no person shall be subject to any penalty for failing to comply with a collection of information if it does not display a currently valid OMB control number.

PLEASE DO NOT RETURN YOUR FORM TO THE ABOVE ADDRESS.

1. REPORT DATE (DD-MM-YYYY) July 2012		2. REPORT TYPE Final		3. DATES COVERED (From - To) May 2011 to May 2012	
4. TITLE AND SUBTITLE Health Assessment and Fault Classification of Roller Element Bearings				5a. CONTRACT NUMBER	
				5b. GRANT NUMBER	
				5c. PROGRAM ELEMENT NUMBER	
6. AUTHOR(S) Andrew J. Bayba, David N. Siegel, Kwok Tom, and Derwin Washington				5d. PROJECT NUMBER 2NE6KK	
				5e. TASK NUMBER	
				5f. WORK UNIT NUMBER	
7. PERFORMING ORGANIZATION NAME(S) AND ADDRESS(ES) U.S. Army Research Laboratory ATTN: RDRL-SER-E 2800 Powder Mill Road Adelphi, MD 20783-1197				8. PERFORMING ORGANIZATION REPORT NUMBER ARL-TR-6080	
9. SPONSORING/MONITORING AGENCY NAME(S) AND ADDRESS(ES)				10. SPONSOR/MONITOR'S ACRONYM(S)	
				11. SPONSOR/MONITOR'S REPORT NUMBER(S)	
12. DISTRIBUTION/AVAILABILITY STATEMENT Approved for public release; distribution unlimited.					
13. SUPPLEMENTARY NOTES					
14. ABSTRACT Feature extraction, health assessment, and fault classification algorithms were evaluated for ball bearings with three different fault types and multiple levels of damage. Data was analyzed for five healthy bearings, and seeded fault bearings with five levels of damage for each fault type (ball fault, inner race fault, and outer race fault). A variety of fault analysis techniques were used to calculate properties (features) of the data sets, which were then fused together to form the best feature sets for fault evaluation. Self-organizing maps were used for health assessment, and a Naïve Bayes classifier was used to determine fault type. The results indicate a very good distinction between healthy and faulted bearings, and a good classification of fault types. For health assessment, there were good general trends with increasing damage. There was, however, a significant amount of scatter, thereby making it difficult to ascertain the precise health of an individual bearing. Although our feature set is substantial, it is by no means exhaustive, and one consideration is to seek additional features that may produce a higher level of confidence in individual bearing health.					
15. SUBJECT TERMS Bearing health assessment, bearing fault classification, roller element bearings, seeded fault testing					
16. SECURITY CLASSIFICATION OF:			17. LIMITATION OF ABSTRACT UU	18. NUMBER OF PAGES 24	19a. NAME OF RESPONSIBLE PERSON Andrew J. Bayba
a. REPORT Unclassified	b. ABSTRACT Unclassified	c. THIS PAGE Unclassified			19b. TELEPHONE NUMBER (Include area code) (301) 394-0440

Contents

List of Figures	iv
List of Tables	iv
1. Introduction	1
2. Bearings Under Test	1
3. Test Equipment and Instrumentation	3
4. Data	5
5. Analysis	6
5.1 Feature Extraction	6
5.2 Feature Selection	8
5.2.1 For Health Assessment	8
5.2.2 For Fault Classification	9
5.3 Health Assessment	10
5.4 Fault Classification.....	10
6. Results	11
7. Discussion and Conclusions	14
8. References	16
List of Symbols, Abbreviations, and Acronyms	17
Distribution List	18

List of Figures

Figure 1. Cross section of a ball bearing with nominal seeded fault locations.....	2
Figure 2. Test rig used in performing bearing experiments.	4
Figure 3. Mounting locations and orientation of the accelerometers.....	5
Figure 4. Health assessment and fault classification process.	6
Figure 5. Bearing health value as a function of the outer race damage level.	12
Figure 6. Bearing health value as a function of the inner race damage level.	13
Figure 7. Bearing health value as a function of the ball damage level.	14

List of Tables

Table 1. Defect frequencies for the bearings.	3
Table 2. Data sets.	5
Table 3. Extracted features and methodology.....	8
Table 4. Top features for health assessment.	9
Table 5. Top features for fault classification.	10
Table 6. Classification of fault types (confusion matrix).	14

1. Introduction

The United States Army has a substantial interest in the application of prognostics and diagnostics (P&D) for components and systems. The interest is two-fold; the commander in the field has an intense interest in operational readiness of assets, while logistical personnel are interested in cost efficiency. These can both be optimized by providing an accurate real-time health assessment and remaining useful life (RUL) prediction. As a result of these needs, the U.S. Army Research Laboratory (ARL) has been actively pursuing advancements in P&D. Bearings are of particular interest because of their existence in virtually every Army system, and the consequent requirement for a large amount of effort dedicated to monitoring them with the hope that they are being maintained or replaced at the best time.

Health assessment algorithms have been under development at ARL using a variety of parameters or “features” extracted from several signal processing techniques commonly accepted in the assessment of bearing health. This report focuses on the application of these algorithms to the results of seeded fault bearing tests, both for evaluation and improvement purposes. We use vibration signals from accelerometers mounted in the vicinity of the bearing as the monitoring source for our analysis/feature extraction. The uniqueness of this work is in the fusion of a variety of features/signal processing techniques with the belief that this wide collection of features will provide a better likelihood of capturing any degradation in a bearing and, thus, produce a more accurate health assessment. In all, there are 288 features used in the signal processing—72 individual features for each of four accelerometer channels. The features range from simple statistics, such as root mean square (RMS), to rather complex items, such as Wavelet Band Energy. The testing procedure and data collected are described in reference 1.

2. Bearings Under Test

All the bearings used in this study were Rexnord ER16K ball bearings. All of the bearings were new and most had defects intentionally made in them (seeded faults). There were five good bearings and 15 bearings with seeded faults. The faulted bearings consisted of five bearings with ball faults, five bearings with inner race faults, and five bearings with outer race faults. The bearings of each fault type had five levels of damage of the specific defect. Figure 1 is a cross-section of a bearing showing nominal locations of the seeded faults along with their associated components. The bearings were provided as a custom order from SpectraQuest, Inc., who was also responsible for applying the faults to the bearings. The bearing parameters are presented here along with the bearings characteristic frequencies (commonly referred to as fault frequencies or defect frequencies).

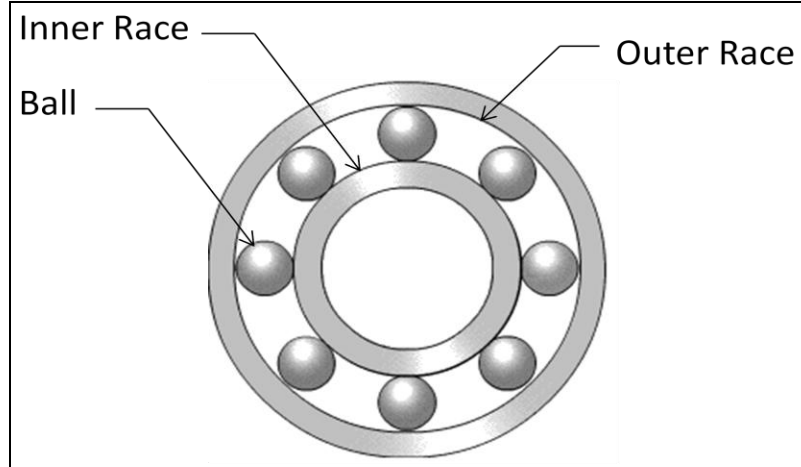


Figure 1. Cross section of a ball bearing with nominal seeded fault locations.

For these experiments, the bearing parameters are:

Number of balls, $n = 9$

Ball Diameter, $BD = 0.3125$ in

Pitch Diameter, $PD = 1.5157$ in,

Contact angle, $\theta = 0$

Operating frequency, $f = 35$ Hz

The formulae for the defect frequencies are:

$$BPFI = \frac{n}{2} \left(1 + \frac{BD}{PD} \cos \theta\right) * f \quad (1)$$

$$BPFO = \frac{n}{2} \left(1 - \frac{BD}{PD} \cos \theta\right) * f \quad (2)$$

$$FTF = \frac{1}{2} \left(1 - \frac{BD}{PD} \cos \theta\right) * f \quad (3)$$

$$Rolle = \frac{PD}{BD} \left(1 - (BD/PD)^2 \cos^2 \theta\right) * f \quad (4)$$

$$BSF = \frac{PD}{2BD} \left(1 - (BD/PD)^2 \cos^2 \theta\right) * f \quad (5)$$

where

Ball pass frequency inner (BPFI) = the frequency corresponding to a defect on the inner race.

BPFO = the ball pass frequency of the outer race and corresponds to a defect on the outer race.

FTF = the fundamental train frequency, i.e., the frequency of the cage.

BSF = the ball spin frequency, i.e., the rotational frequency of each ball.

Rolle = the ball defect frequency; (Rolle = 2 x BSF; a ball defect will strike one of the races at this frequency).

The calculated values of the defect frequencies are listed in table 1.

Table 1. Defect frequencies for the bearings.

BPMI	BPFO	FTF	BSF	Rolle
190 Hz	125 Hz	13.9 Hz	81.3 Hz	162.5 Hz

3. Test Equipment and Instrumentation

The bearings were placed in service on a test rig manufactured by SpectraQuest Inc. (figure 2). The rig is specifically designed for studying defects in machine components and is outfitted with mounting holes for accelerometers in positions of interest. As can be seen in figure 1, the rig is a complete drivetrain consisting of an electric motor; shaft with weights, pulleys, and belts; a gearbox; and a magnetic load. The shaft was supported by two ball bearings near the ends of the shaft. The bearing closest to the motor was the bearing under test, while the bearing further from the motor was always a known good bearing. The shaft was loaded with two 11-lb cylindrical weights that rotate with the shaft; one on either side of the bearing under test. For this study, the belts, gearbox, and magnetic load were removed from the drivetrain to reduce the noise from vibrations not related to the bearings.



Figure 2. Test rig used in performing bearing experiments.

The test rig was instrumented with a tachometer (supplied with the test rig) and two triaxial accelerometers, manufactured by Vibra-Metrics, Inc. Both accelerometers were attached to the mounting block of the bearing under test: one directly above the bearing and one to the side of it, at 90° to the first accelerometer. The accelerometer placements and axis orientations are shown in figure 3. The x-axes of both accelerometers point in the axial direction of the system—i.e., parallel to the shaft axis—while the z- and y-axes point in radial directions—i.e., perpendicular to the axis of the shaft. All accelerometer channels were active and connected to the data acquisition system; however, due to the high sampling rate (100 KSamples/s/channel), only four channels could be collected. All channels of the first accelerometer were collected, and the x direction channel of the second accelerometer was selected for collection because it had a higher amplitude return than the y and z directions.

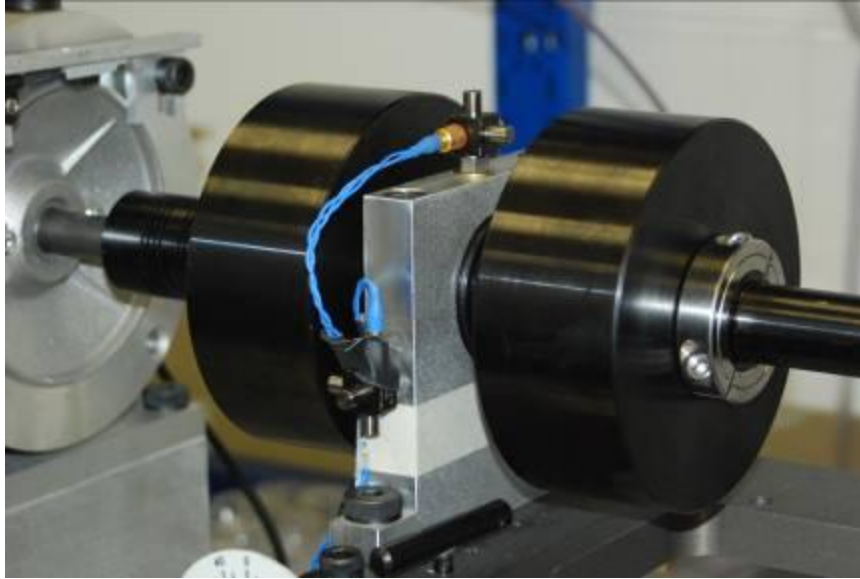


Figure 3. Mounting locations and orientation of the accelerometers.

4. Data

The data was collected from the tachometer and accelerometers for 10 runs of each of the 20 bearings investigated. Data from the tachometer was not used in this study and will not be discussed further here; however, it was retained since it may prove useful in future studies. The accelerometer data was collected in the units of g's of acceleration. The data, as collected, was in the binary format of the DAQ hardware and was slightly over 10 s for each run. Exactly 10 s of the accelerometer data was extracted from each of these files and was written to ASCII text files as four columns of tab delimited data, one column for each accelerometer channel. The data is summarized in table 2.

Table 2. Data sets.

Data Set	# Files
Healthy Bearings	50 (10 for each bearing)
Inner Race Defect	50 (10 at each level)
Outer Race Defect	50 (10 at each level)
Ball Defect	50 (10 at each level)

5. Analysis

The analysis involved the application of several ARL-developed algorithms to extract features from the data, select the most useful features, assess the health of the bearings, and identify the fault type of a particular bearing. MATLAB was used for algorithm development and data processing. The ARL algorithms include the use of MATLAB built in functions, as well as algorithms developed by the Center for Intelligent Maintenance Systems, a consortium of the University of Cincinnati, the University of Michigan, and Missouri University of Science and Technology. The algorithms developed at ARL will be described in general here. The flow of the analysis is depicted in figure 4, and is followed by a description of the steps.

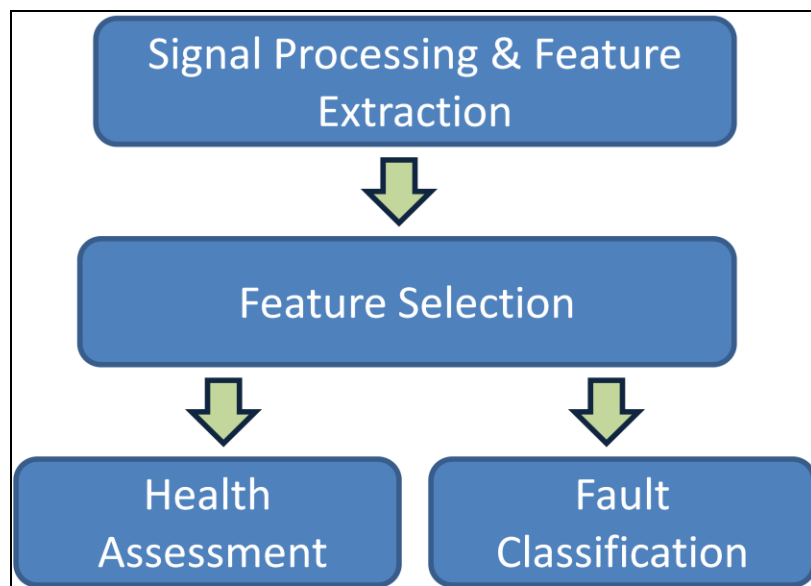


Figure 4. Health assessment and fault classification process.

5.1 Feature Extraction

Characteristics of the signals, commonly referred to as features, were calculated from the data files. A significant amount of research into bearing fault feature generation has been conducted over the last few decades. Features deemed useful for this study were determined based on a review of the literature. A large selection of features was included, providing a greater likelihood that a defect would be identified and also that this work may reveal which features are of greater value for these defect types. In all there were 288 features calculated per run (72 per channel for each run). The features are described further, along with rationale for using them in table 3.

- a. Time Domain Statistics. Statistics of the signals in the time domain were extracted. They are easy to calculate, making them amenable to application in the field, and they are known to vary with fault level, although not always with high correlation. An additional set of statistical features was created by first lowpass filtering the data prior to the calculations, with the intent of noise reduction. The filter was a fourth-order lowpass Butterworth filter with a cut-off frequency of 1500 Hz.
- b. FFT Band Energy. It is typical that there is a shift in spectral energy with bearing degradation. To capture this effect as features, the frequency spectrum was divided into four KHz Bands and the energy in each of these bands was calculated for each signal.
- c. FFT Bearing Fault Frequency Energy. As defects appear and develop, the bearing's defect frequencies often grow in amplitude. The actual defect frequencies will vary slightly from those presented in table 1 due to slippage. Therefore, small bands (± 2 Hz) around the calculated frequencies were used. The largest peak within each of the bands produced the features.
- d. Bearing Envelope Analysis. The bearing defect frequencies are often masked by noise and other spectral content at their true, relatively low, calculated frequencies. To aid in isolating them, high frequency envelope analysis is commonly employed (2). The technique involves determining a suitable frequency band, where the signal is amplified. We examined several frequency bands and found that the band where the spectral kurtosis was highest worked well. The technique then employs demodulating the band pass filtered signal and applying the methodology of item c. to produce the features.
- e. Spectral Kurtosis. Kurtosis as a function of frequency highlights which frequency band shows the most variation in the signal, being related to the impact of the bearing against the defect, and provides a good characterization of a signal (3, 4). We sum the kurtosis values in different bands and use them as features.
- f. Discrete Wavelet Transforms (DWT). Wavelet transforms employ a waveform shape that is better matched to a transient, impulsive response that is typical of these types of defects where periodic impacts occur. Using wavelet decomposition, the signal was evaluated at different decomposition levels to establish the level that provides the best correlation to the damage level. In this case, level 9 decomposition was performed, and the energy at each level was calculated. The energy at approximation and detail filters were normalized as a percentage of total signal energy to produce the features.

Table 3. Extracted features and methodology.

Signal Processing Method Name	Description	# of Extracted Features
Time Domain Statistics	Calculate RMS, Kurtosis, Peak to Peak (P2P), Crest Factor, and Variance	40 (10 each signal)
FFT Band Energy	Calculate energy in Frequency Spectrum in bands of 4kHz	40 (10 each signal)
FFT Bearing Fault Frequency Energy	Calculate amplitude information at bearing fault frequencies	48 (12 each signal)
Bearing Envelope Analysis	Demodulates band pass filtered signal to better extract information at bearing fault peaks	100 (25 each signal)
Spectral Kurtosis	Kurtosis value in different frequency bands	20 (5 each signal)
Discrete Wavelet Transform	Calculates energy at approximation and details as % of total signal energy	40 (10 each signal)

5.2 Feature Selection

5.2.1 For Health Assessment

To select the most useful features for health assessment, correlation of individual features with fault level was performed and ranked. The top five features were used for the health assessment algorithm. For reference, the top 20 features for each fault type are provided in table 4, where x-1,y-1,z-1 and x-2 in the feature name identify which accelerometer (1 or 2) and direction the signal is associated with. Note that the top features come from nearly all of the feature extraction techniques, emphasizing the value in employing a variety of techniques.

Table 4. Top features for health assessment.

Inner Race Faults	Outer Race Faults	Ball Faults
'P2P LowPass y-1'	'Details Level 8 y-1'	'P2P LowPass y-1'
'RMS LowPass y-1'	'P2P x-1'	'Crest Factor LowPass y-1'
'P2P z-1'	'Details Level 9 y-1'	'Crest Factor x-1'
'P2P y-1'	'y-1 FFT Band Energy from 24001 Hz to 28000 Hz'	'Crest Factor LowPass z-1'
'SpecKurtBand5 y-1'	'y-1 FFT Band Energy from 20001 Hz to 24000 Hz'	'P2P x-2'
'SpecKurtBand5 x-2'	'Details Level 8 x-2'	'P2P LowPass z-1'
'P2P x-2'	'z-1 FFT Band Energy from 20001Hz to 24000Hz'	'Details Level 7 x-2'
'z-1 FFT Band Energy from 24001 Hz to 28000 Hz'	'x-2 FFT Band Energy from 20001 Hz to 24000 Hz'	'Kurtosis LowPass z-1'
'Kurtosis x-2'	'RMS y-1'	'x-2 FFT Band Energy from 1 Hz to 4000 Hz'
'RMS z-1'	'Kurtosis x-1'	'Crest Factor x-2'
'Variance_LowPass y-1'	'y-1 FFT Band Energy from 1 Hz to 4000 Hz'	'x-2 FFT Band Energy from 8001 Hz to 12000 Hz'
'SpecKurtBand5 x-1'	'P2P x-2'	'Kurtosis x-2'
'P2P x-1'	'RMS x-2'	'Crest Factor y-1'
'x-1 FFT Band Energy from 32001 Hz to 36000 Hz'	'Kurtosis LowPass z-1'	'Kurtosis y-1'
'x-1 FFT Band Energy from 28001 Hz to 32000 Hz'	'P2P Envelope z-1'	'P2P Envelope x-2'
'RMS LowPass z-1'	'P2P Envelope y-1'	'Kurtosis LowPass y-1'
'Crest Factor x-1'	'Details Level 5 y-1'	'SpecKurtBand1 x-2'
'P2P Envelope x-2'	'x-2 FFT Band Energy from 1 Hz to 4000 Hz'	'BSF_Energy y-1'
'RMS Envelope x-2'	'P2P LowPass z-1'	'Crest Factor LowPass x-2'
'RMS LowPass x-2'	'Details Level 9 x-2'	'BSF_Energy z-1'

5.2.2 For Fault Classification

For selecting appropriate features for fault classification, a wrapper method was used. A Naïve Bayes classifier was used as the classification algorithm to which the wrapper feature selection technique was applied. Naïve Bayes classification will be described in more detail later in this report. In the wrapper method, a forward selection process is done, in which a new feature is added only if it provides noticeable improvement in the classification results. The output of the wrapper technique contains the best features to include in the classification analysis (5). The top features are listed in table 5.

Table 5. Top features for fault classification.

'RMS x-1'
'Kurtosis x-1'
'P2P LowPass x-1'
'Crest Factor y-1'
'Variance y-1'
'RMS LowPass y-1'
'Kurtosis LowPass y-1'
'Crest Factor z-1'
'Variance x-2'
'RMS LowPass x-2'
'x-1 FFT Band Energy from 20001 Hz to 24000 Hz'
'z-1 FFT Band Energy from 4001 Hz to 8000 Hz'
'x-2 FFT Band Energy from 36001 Hz to 40000 Hz'
'Details Level 1 x-1'
'Details Level 7 y-1'
'Details Level 4 y-1'
'Details Level 2_y-1'
'SpecKurtBand5 x-1'

5.3 Health Assessment

A Self Organizing Map (SOM) algorithm was used to assess the health of the bearings. This method was selected because it only requires baseline (healthy) data for training the algorithm. The main concept is that the algorithm clusters good data, and as data sets from bearings in question come in, their health is calculated based on proximity of their features to the features of healthy bearings. More specifically, the algorithm calculates a health value for each bearing based on the Euclidian distance from the healthy training data based on multiple features (6, 7). The algorithm was trained with the top features from half of the healthy bearings. The features from the remaining healthy bearings and from the fault cases were used to evaluate the performance of the algorithm since the actual states of health were known.

5.4 Fault Classification

A Naïve Bayes classifier was used to identify the fault types of individual bearings. The technique is based on Bayes law, which relates the probability of an event (fault type) occurring on evidence (the vibration features). The method uses training data to determine the probabilities of having features in a certain range given the bearing fault type (including no fault/healthy). The classifier was trained with healthy data sets and all representative fault types. The trained model is then used to calculate the probability of a bearing under investigation of being in each class (fault type), given the feature values. It then simply chooses the most probable fault type. For continuous values, such as the vibration features, one may assume a distribution for the features; in our case, we assumed a Gaussian distribution. Effectively, this means that for each fault type, a mean and standard deviation were estimated and a Gaussian distribution was fit using the training data. When a test sample comes in, the Gaussian distribution is used to estimate the

probability of each fault type given that feature value. Since there are multiple features, a product formulation is used by multiplying the probabilities together. The classifier performs this probability calculation for each fault type and selects the most probable type. Cross validation was performed to randomly split up the data set into a training set and a test set for evaluation purposes. Advantages of this technique are that it is very straightforward and simple to apply, it is intuitive, it can be applied for classification problems with multiple classes, it and works reasonably well. The disadvantage is that an assumption of independent features is not always met; consequently, more sophisticated methods might perform slightly better (although they could be prone to over-fitting). Also, some classification algorithms, such as support vector machines, are only designed for binary classification (good/bad) and are more cumbersome to use for multiple classes (healthy, inner, outer, ball, etc.).

6. Results

The results, in general, are quite good. Plots of health vs. damage level for the bearings are presented for the three different fault levels in figures 5–7, where a higher value on the vertical axis indicates reduced health. The results indicate that a damaged bearing can easily be distinguished from a healthy bearing for all fault types and all fault levels, and that the calculated health values have an upward trend with the level of damage. There are two points of concern to be noted with the health values. First, there is a significant amount of scatter in many of the health values, particularly with the ball faults. Second, the health value for fault level 3 is better than for fault level 2 on the inner race fault plot (figure 6). Both of these items will be addressed in the Discussion and Conclusions Section. The results indicate that classification of the fault type is for the most part very good, with correct classification of healthy, inner race, and outer race faults 100% of the time and correct classification of ball faults approximately 75% of the time. The fault classification results are presented in table 6 as a confusion matrix, as is common. The table presents the “predicted” classification of each of the runs of a given fault type (50 healthy files and 50 files for each fault type). For example, 13 of the ball fault cases were misclassified as inner race faults and 37 of the ball fault cases were correctly classified. The ball faults present poorer results for both damage level vs. calculated health and fault type classification. This is not unexpected due to the high degree of randomness in which the damage on the ball makes contact with the other components, coupled with the short duration of the impact when contact is made.

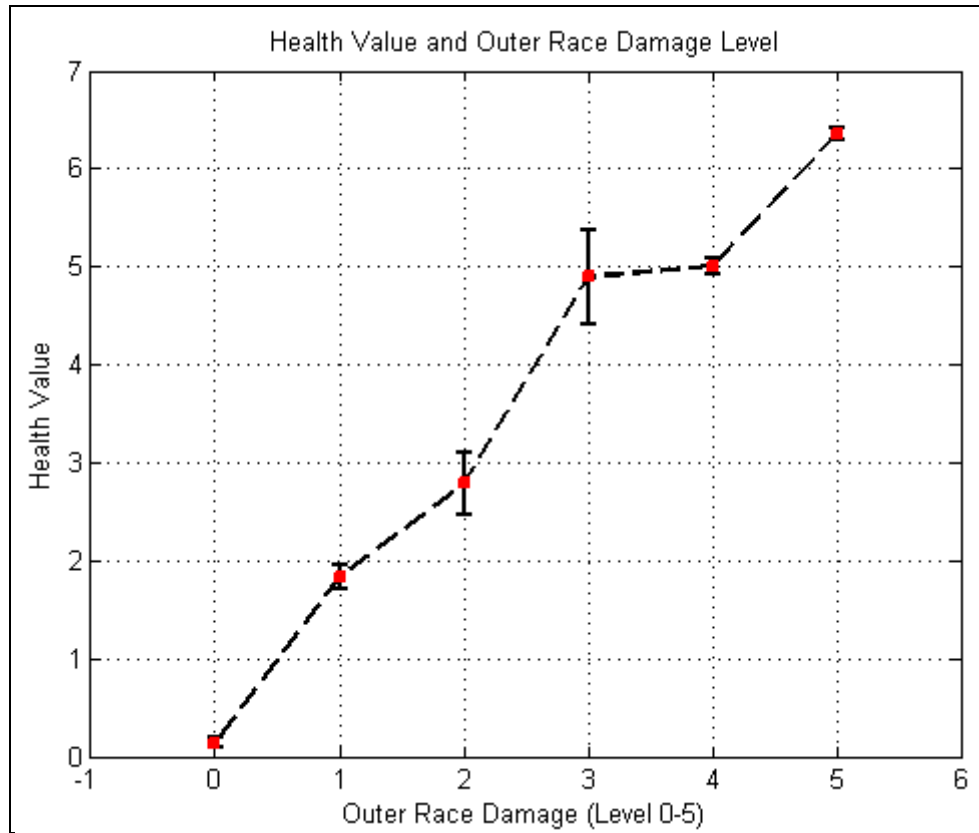


Figure 5. Bearing health value as a function of the outer race damage level.

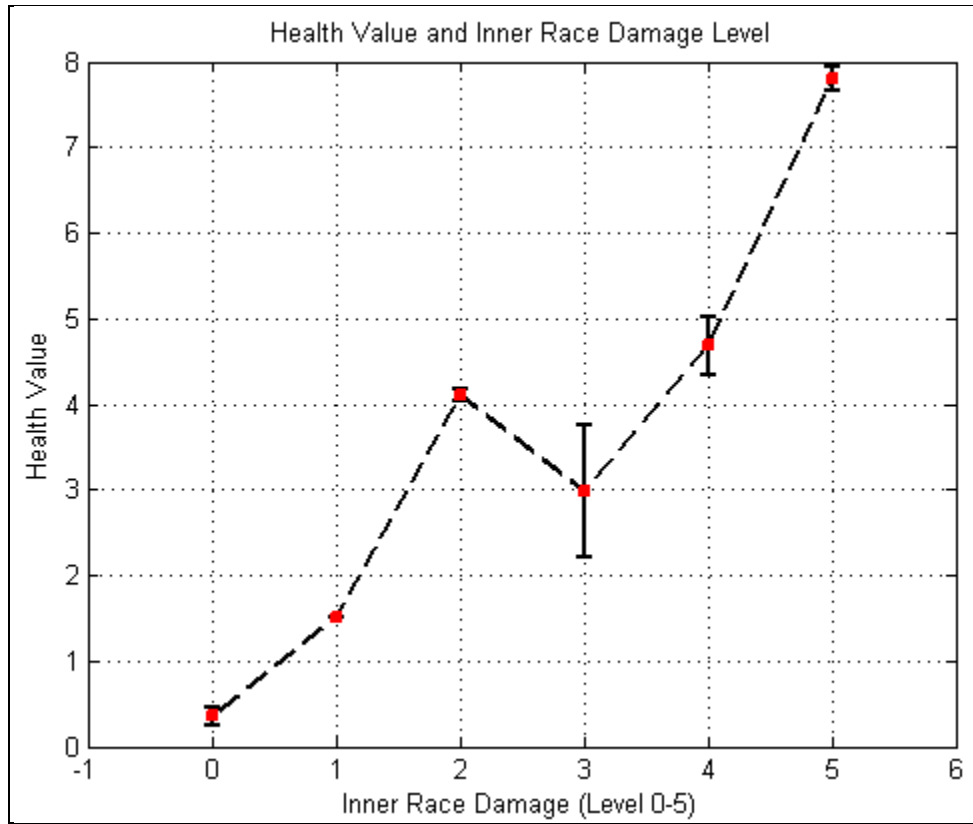


Figure 6. Bearing health value as a function of the inner race damage level.

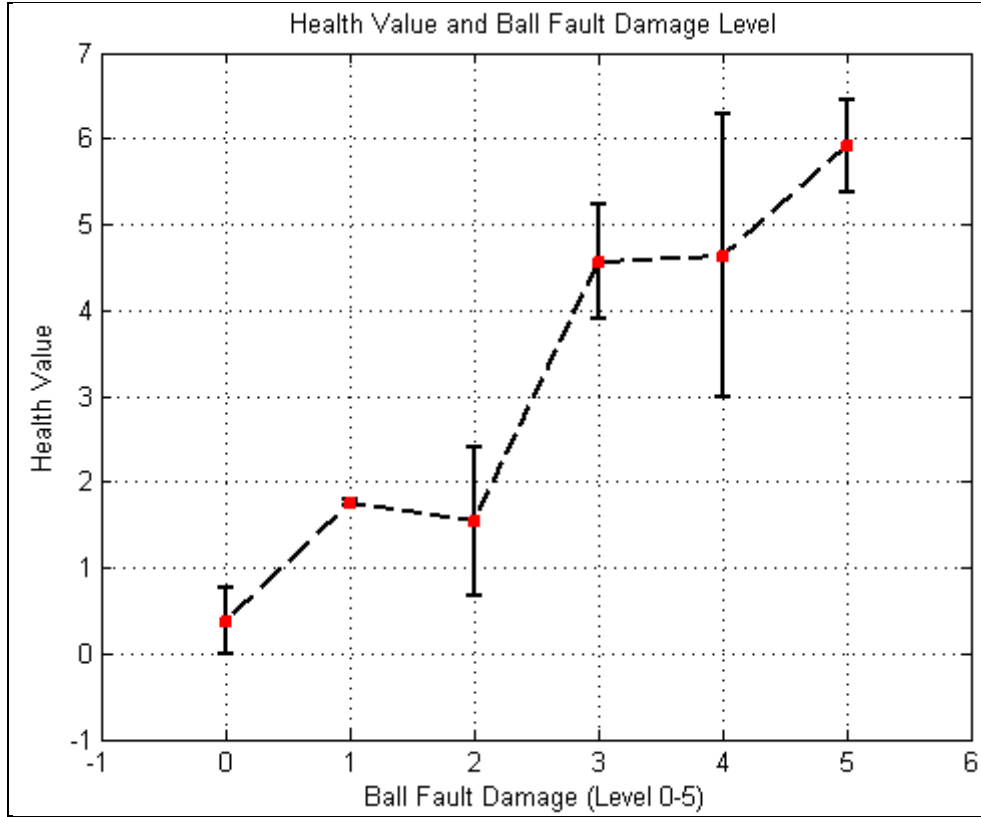


Figure 7. Bearing health value as a function of the ball damage level.

Table 6. Classification of fault types (confusion matrix).

		Predicted			
		Healthy	Inner	Outer	Ball
Actual	Healthy	50	0	0	0
	Inner	0	50	0	0
	Outer	0	0	50	0
	Ball	0	13	0	37

7. Discussion and Conclusions

Algorithms have been developed that may be used to predict the health and fault type of a monitored bearing. Although the algorithms focus on inner race, outer race, and ball faults, they could be easily adapted to additional fault types. The algorithm for fault type classification works very well with some exception to ball faults. Misclassification of about 25% of the ball faults is almost certainly due to the randomness in which how and when the damage on the ball strikes the races. It is recommended that an improved set of features be examined for this application. Also, some code development work needs to be done to eliminate some randomness in the selection of the top features, which has been seen to have an effect on the results. The health

assessment algorithm can be used to assess the health of a bearing. It always correctly shows whether or not there is some level of damage. The confidence in the health value for certain fault types and fault levels is questionable. The issue is in variability of the feature values at those particular fault levels/types and hence health assessment values. Use of a larger data set should greatly improve the problem. One curious item is that fault level 3 appears to be healthier than fault level 2 for the inner race. It is believed that this may very well be the case as many of the features were examined and all appear to provide the same result. Unfortunately, the engineer who produced the faults is no longer available for discussion of the issue. It may simply be a matter of mislabeling. It is significant to note that the top features for both health assessment and fault classification come from nearly all of the feature extraction techniques, emphasizing the value in incorporating a variety of techniques. Finally, it is believed that significant improvements could be attained by enhancements in processing techniques, incorporating additional features, and tuning and optimizing the code.

8. References

1. Bayba, A.; Washington, D.; Tom, K. *Seeded Fault Bearing Experiments: Methodology and Data Acquisition*; ARL-TR-5575; U.S. Army Research Laboratory: Adelphi, MD, 2011.
2. McFadden, P. D.; Smith, J. D. Vibration Monitoring of Rolling Element Bearings by High Frequency Resonance Technique. *A Review, Tribology International* **1984**, *77*, 3–10.
3. Antoni, J. The Spectral Kurtosis: A Useful Tool for Characterizing Nonstationary Signals. *Mechanical Systems and Signal Processing* **2006**, *20*, 282–307.
4. Antoni, J.; Randall R. B. The Spectral Kurtosis: Application to the Vibratory Surveillance and Diagnostics of Rotating Machines. *Mechanical Systems and Signal Processing* **2006**, *20*, 308–331.
5. Guyon, I.; Elisseeff, A. An Introduction to Variable and Feature Selection. *The Journal of Machine Learning Research* **2003**, *3*, 1157–1182.
6. Kohonen T.; Oja E., Simula O.; Visa, A.; Kangas J. Engineering Application of the Self-Organizing Map. *Proceedings of the IEEE* *84* (10) pp. 1358–1384, 1996.
7. Qiu, H.; Lee, J.; Ling, J.; Yu, G. Robust Performance Degradation Assessment Method for Enhanced Rolling Element Bearings Prognostics. *Journal of Advanced Engineering Informatics* **2003**, *17*, 127–140.

List of Symbols, Abbreviations, and Acronyms

ARL	U.S. Army Research Laboratory
BD	ball diameter
BPFI	ball pass frequency inner
DWT	Discrete Wavelet Transforms
PD	pitch diameter
P&D	prognostics and diagnostics
RMS	root mean square
RUL	remaining useful life
SOM	Self Organizing Map

NO. OF COPIES	ORGANIZATION	NO. OF COPIES	ORGANIZATION
1 ELEC	ADMNSTR DEFNS TECHL INFO CTR ATTN DTIC OCP 8725 JOHN J KINGMAN RD STE 0944 FT BELVOIR VA 22060-6218	1 (PDF ONLY)	NASA GLENN US ARMY RESEARCH LAB ATTN RDRL VTP H DECKER BLDG 23 RM W121 CLEVELAND OH 44135-3191
1	US ARMY RSRCH DEV AND ENGRG CMND ARMAMENT RSRCH DEV & ENGRG CTR ARMAMENT ENGRG & TECHNLY CTR ATTN AMSRD AAR AEF T J MATTS BLDG 305 ABERDEEN PROVING GROUND MD 21005-5001	3 (PDF ONLY)	US ARMY TARDEC ATTN RDTA RS C BECK ATTN RDTA RS K FISHER ATTN RDTA RS S HUSSAIN MS# 204 6501 E 11 MILE RD WARREN MI 48397-5000
1	US ARMY INFO SYS ENGRG CMND ATTN AMSEL IE TD A RIVERA FT HUACHUCA AZ 85613-5300	1 (PDF ONLY)	USAMSAA ATTN T. S. KILBY 392 HOPKINS RD APG MD 21005
1	US GOVERNMENT PRINT OFF DEPOSITORY RECEIVING SECTION ATTN MAIL STOP IDAD J TATE 732 NORTH CAPITOL ST NW WASHINGTON DC 20402		
7	US ARMY RSRCH LAB ATTN IMNE ALC HRR MAIL & RECORDS MGMT ATTN RDRL CIO LL TECHL LIB ATTN RDRL CIO LT TECHL PUB ATTN RDRL SER E A BAYBA ATTN RDRL SER E D SIEGEL ATTN RDRL SER E D WASHINGTON ATTN RDRL SER E K TOM ADELPHI MD 20783-1197		
4 (PDF ONLY)	DIRECTOR US ARMY RESEARCH LAB ATTN RDRL VTM M HAILE ATTN RDRL VTM A GHOSHAL ATTN RDRL VTM M MURUGAN ATTN RDRL VTP B DYKAS BLDG 4603 APG MD 21005		